Journal of Structural Geology, Vol. 12, No. 4, pp. 403 to 417, 1990
Printed in Great Britain

0191-8141/90 $03.00+0.00

Strain fabric associated with the Meade thrust sheet: implications for cross-section balancing

GRETCHEN M. PROTZMAN

Department of Geology, University of California, Davis, CA 95616, U.S.A.

and

GAUTAM MITRA

Department of Geology, University of Rochester, Rochester, NY 14627, U.S.A.

(*Received* 29 *June* 1989; *accepted in revised form* 16 *January* 1990)

Abstract—Emplacement of the Meade thrust sheet, southeastern Idaho, U.S.A., was accompanied by the development of a strain fabric and significant footwall deformation. Characteristics of the strain fabric are based on strain estimates using pressure-solution cleavage and deformed fossils within the Jurassic Twin Creek Formation. The strain fabric formed during early layer-parallel shortening at the thrust front and accommodates from 10 to 35% shortening within the incipient thrust sheet. Footwall strata were later folded above a detachment at the base of the Twin Creek Formation, and the early strain fabric was passively rotated. The structural development of this area, consisting of (1) strain fabric development, (2) folding of the footwall and (3) the truncation of footwall structures by imbricates of the Meade thrust, are placed in a relative time frame to aid in section reconstruction. The passive reorientation of the strain fabric and the truncation and incorporation of footwall structures into the thrust sheet are used as kinematic and geometric constraints for cross-section balancing. We present a sequential retrodeformation of the Meade thrust sheet in which strain is removed from the cross-section at the appropriate geometric stages in the deformation. These sections illustrate some methods by which strain data can be incorporated into cross-sections and also indicate the difficulty involved in balancing cross-sections of internally deformed thrust sheets. Interpretation of these sections suggests that a significant amount of footwall deformation accompanied the emplacement of the Meade thrust sheet and that footwall deformation is strongly controlled by the local stratigraphic package. The sections also illustrate that the earliest deformation within a thrust sheet may be unrelated to motion on the underlying incipient thrust, and that the trace of a thrust fault which cuts previously deformed strata will not restore to a typical ramp and flat geometry.

INTRODUCTION

THE methods of balancing cross-sections have become a standard approach for interpreting the structures of fold and thrust belts. For the external portions of fold and thrust belts, the simple assumptions of plane strain deformation and parallel folding in which both bed length and bed area are conserved (Dahlstrom 1969) result in sections that reflect the style of the "foothills family of structures". In the internal portions of a thrust belt, however, fold styles become more complex, and lithology as well as deformation conditions play an increasingly important role in the structural development of individual thrust sheets. The structural style of these sheets can not be reproduced accurately using simplifying geometric constraints; therefore, section balancing and restoration become more difficult for the internal portions of thrust belts. In such cases, substantially more detailed information is required to produce a viable cross-section. Such data typically include down-plunge projections, kinematic information, detailed field information on geometry and the relative timing of various small-scale structures, and finite and incremental strain data. In this paper, we discuss our approach toward the incorporation of these types of information into the cross-section balancing technique.

The idea that the structures resulting from a well-constrained deformation event can be retrodeformed step-by-step from the final to the initial state is fundamental to the idea of cross-section balancing. For frontal thrust sheets this step-wise retrodeformation is the reasoning behind the "pin and pull-back" balancing technique. More complexly deformed thrust sheets can also be retrodeformed by an incremental process (Protzman & Mitra 1985, Cooper & Trayner 1986), provided that additional geometric and kinematic constraints (e.g. the geometry of complex folds in the hanging wall and footwall adjacent to the thrust, the geometry of folded fault surfaces, and the characteristics of any strain within the thrust sheet) are used in the restoration.

One concept that we use in this paper is that of a *strain fabric* which is defined by the shape changes of deformed markers and includes information about the spatial orientation and distribution of the strain. The strain fabric can be defined both quantitatively and qualitatively and used as an aid in the retrodeformation and balancing of the cross-section. Clearly the strain fabric can be either homogeneous or inhomogeneous depending upon the nature of the deformation and also on the scale at which it is being studied. Because large quantities of evenly distributed strain data are required to describe the strain fabric in an area completely, most workers do not incorporate strain information into balanced cross-sections. For the scale at which most

cross-sections are drawn, it is possible to restrict our interest to regional variation in two characteristics of the main strain fabric, namely the average strain magnitude and the orientation of the principal directions. Once the regional patterns of these two characteristics of the strain fabric are identified, strain information can be more readily incorporated into sections.

We show an example of the sequential balancing technique as applied to a cross-section through the Meade thrust sheet in the Idaho–Wyoming thrust belt, U.S.A. The Meade thrust sheet was emplaced early in the deformation history of the thrust belt as an internal sheet, and it records a fairly complex history of strain related to fault motion. Critical timing relationships between faults, folds and the development of a strain fabric within the Meade sheet and the adjacent footwall have been the subject of several earlier studies (Mitra *et al.* 1984, Mitra & Yonkee 1985, Protzman 1986). These studies form the framework for our discussion of the emplacement sequence of the Meade thrust sheet.

REGIONAL GEOLOGY

The Idaho–Wyoming thrust belt is a salient of the eastern fold and thrust belt of the North American Cordillera (Fig. 1). The thrust belt developed during the Mesozoic age Sevier Orogeny (Armstrong 1968) and forms a broad arc, convex towards the east. Dominant structural features of the thrust belt are W-dipping low-angle thrust faults that have accommodated eastward transport. Five major thrust sheets have been identified; from the west to east these are the Paris, Meade, Crawford, Absaroka and Darby thrust sheets (Fig. 1). The thrust structures are developed within a thick sedimentary package that was deposited from late Precambrian through to early Tertiary time. Thick synorogenic deposits and cross-cutting relationships between the faults and the sediments have been used to determine the order of emplacement of successive thrust sheets in a relatively well defined time frame. Structures in the thrust belt grow progressively younger from west to east, and involve a younger stratigraphic package to the east indicating that the basal décollement climbed section in the transport direction (Rubey & Hubbert 1959). The stratigraphic and tectonic development of the Idaho–Wyoming thrust belt has been summarized by Armstrong & Oriel (1965), Royse *et al.* (1975) and Wiltschko & Dorr (1983).

In the Idaho–Wyoming thrust belt, both structural complexity and the intensity of strain fabric development increase westward toward the hinterland. The internal sheets of the thrust belt typically contain the more complex structures as these sheets formed first and were modified by later motion on underlying faults. Both the Meade and Crawford thrust sheets are intern-

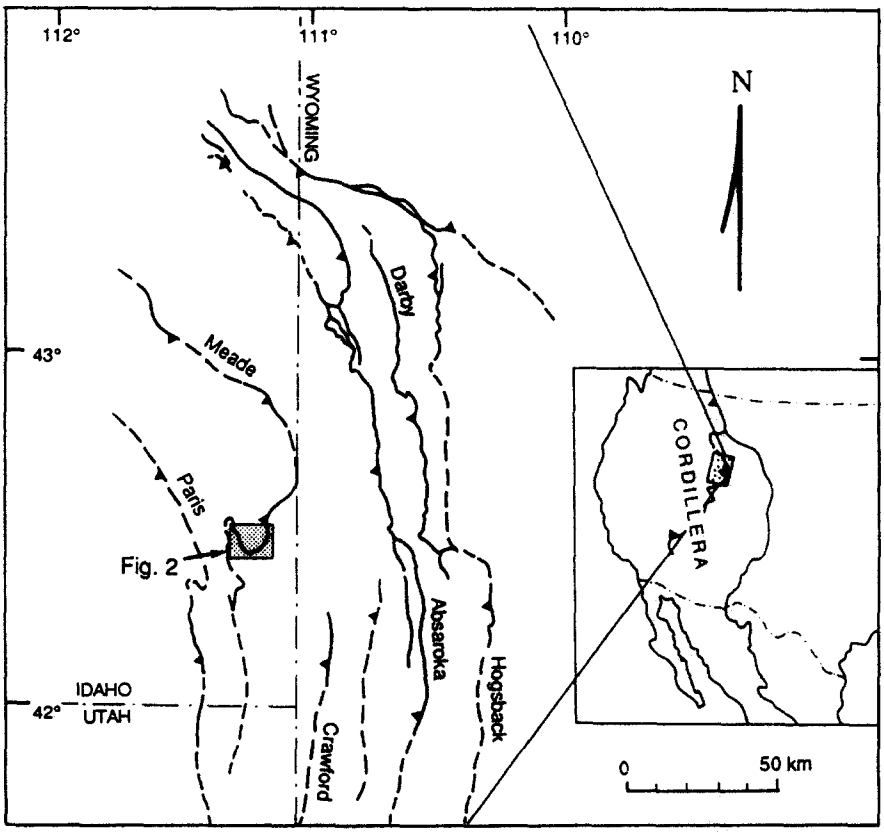

Fig. 1. Location map of the study area (stippled box) within the Idaho–Wyoming thrust belt, U.S.A. Traces of major thrust faults are shown. Stippled area is region shown in Fig. 2.

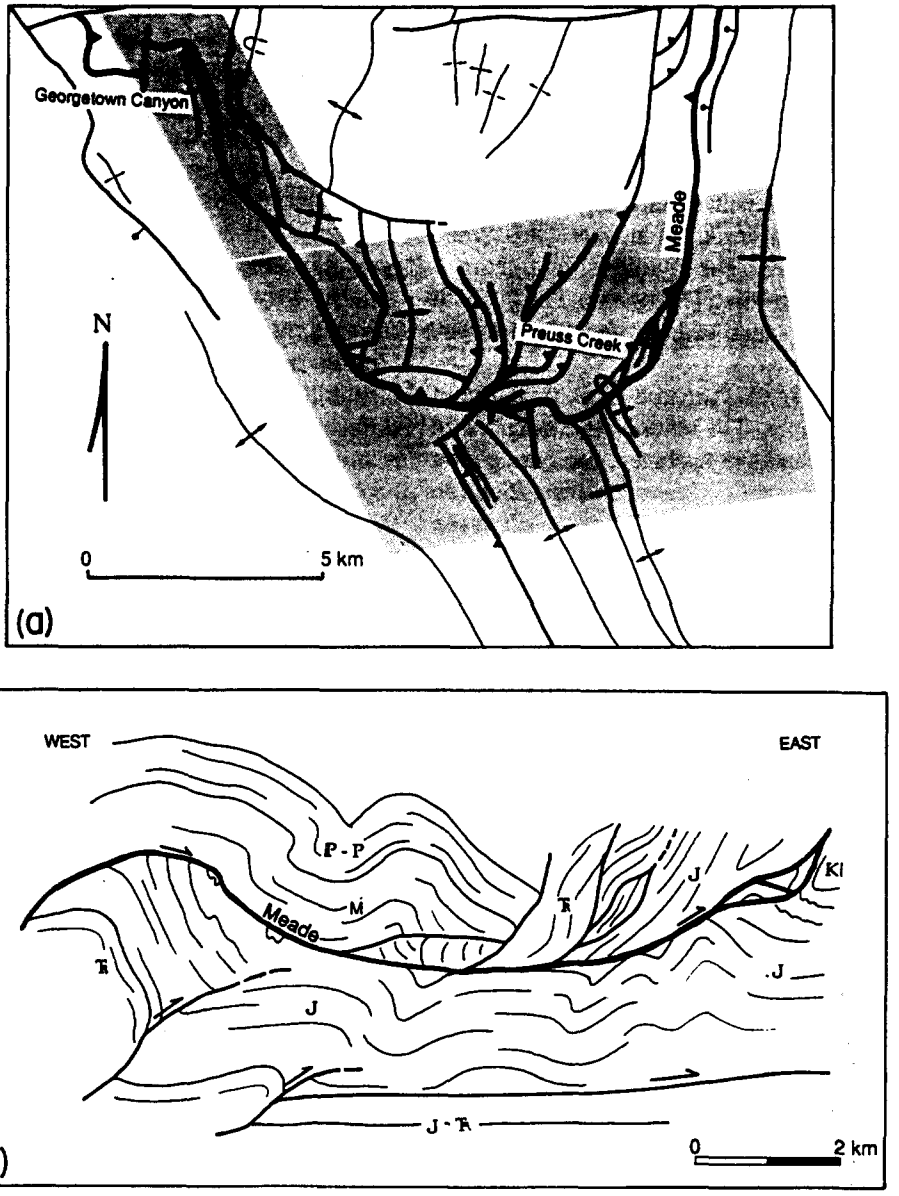

Fig. 2. (a) Structural features at the exposure of the Meade thrust in southeastern Idaho. Shaded area represents region used for down-plunge projection (Fig. 2b). Location of Georgetown Canyon and Preuss Creek localities discussed in the text are indicated. (b) Down-plunge projection of structures in the hanging wall and footwall of the Meade thrust. Ages of strata are indicated. Trend of projection: 07°/352.

ally deformed, although the metamorphic grade associated with the deformation was very low ($T < 200°C$, $P <$ 5 kb, Mitra & Yonkee 1985) and lithologies can be correlated across fault surfaces without difficulty.

We focus our discussion on the structures and strain fabrics associated with the Meade thrust sheet at its exposures in southeastern Idaho (Fig. 2a). These include prominent footwall structures which lie in a broad displacement transfer zone between the Meade and Crawford thrusts as discussed by Evans & Craddock (1985).

STRAIN FABRIC OF THE MEADE THRUST SHEET

Limestones of the Jurassic Twin Creek Formation are exposed in both the hanging wall and footwall of the Meade thrust (Figs. 2b and 3a) and contain strain markers for pressure solution and plastic strains in the form of a penetrative cleavage and deformed fossils. This strain fabric provides information about the individual strain increments and for the relative timing of strain with respect to the formation of mesoscopic structures.

Pressure-solution strain

Two units in the Twin Creek, the Rich and Leeds Creek members (Imlay 1967), are dominantly micritic with 10–20% clay, quartz and feldspar. In these units, a penetrative pressure-solution cleavage that trends NW–SE is well developed and is defined by closely spaced partings, typically oriented at a high angle to bedding (Mitra & Yonkee 1985). Strain estimates, based on the volume per cent of insoluble residue accumulated within the cleavage seams, range from 5 to 20% for bed-parallel

shortening in this area (Yonkee 1983). Tectonic stylolites are more common in the coarsely crystalline limestones of the Twin Creek Formation (Fig. 3b) and follow trends that are parallel to the cleavage seams in the adjacent micritic units. We have estimated minimum shortening strains in a direction perpendicular to the stylolite surfaces from measurements of the average height of stylolite teeth along each surface (Stockdale 1926). Strain estimates from the stylolites range from 3 to 18% bed-parallel shortening (Protzman 1986) which is of the same order of magnitude as the strain determined from the micrites.

Calcite-filled veins (Fig. 3b) are abundant throughout the Twin Creek limestones. The veins both truncate and are truncated by the cleavage surfaces, indicating that they formed at the same time as cleavage. It is difficult to determine the actual volume change due to cleavage formation, although the abundance of vein material coeval with cleavage development suggests that the material removed from the solution surfaces was reprecipitated locally in what may have been a closed system.

Earlier work in this part of the thrust belt discussed the stratigraphic evidence for the timing of cleavage development (Gentry 1983, Mitra *et al.* 1984), and the relationship between cleavage development and the formation of mesoscopic structures in the Meade and Crawford thrust sheets (Mitra & Yonkee 1985). These studies indicate that the cleavage formed during an early increment of layer parallel shortening within the incipient thrust sheet—a deformation that may have been enhanced by the increased temperature and pressures and decreased thermal gradient that resulted from the emplacement of an earlier hotter thrust sheet over the shallower and cooler rocks of the incipient thrust sheet.

Plastic strain

The Leeds Creek member of the Twin Creek Formation contains several discrete, lenticular beds of fossil hash that vary from 2 to 20 cm in thickness. The fossil hash is composed of crinoid stems and dissociated ossicles (crinoid discs) that show the effects of plastic deformation (Fig. 3c). Ossicles from the genus *Pentacrinus* were selected for strain analysis because they originally possessed a pentameral symmetry, and the change from undeformed to deformed state can be measured on the basis of changes in the angles between adjacent rays (Fig. 4a). A simple geometric construction (see Appendix) can be used to determine strain using a Mohr diagram. *Pentacrinus* discs generally lie on the bedding plane and provide two-dimensional strain data for that surface (Fig. 5). In a few horizons, intact *Pentacrinus* stems parallel to bedding are preserved, with discs perpendicular to bedding (Fig. 5). These discs were located by sectioning the fossil-rich layer and were used to estimate strains on planes other than bedding. In studying the deformed shape of ossicles located by sectioning, it is important to be able to recognize and avoid measuring the pseudo-deformed star shapes that result from an oblique cut through a crinoid stem (Fig. 4b). Such oblique sections are indicated by the misorientation of calcite twins across the sutures which separate individual ossicles along the column.

Each crinoid ossicle is composed of a single calcite crystal, and might, therefore, be expected to have a large competency contrast with the extremely fine-grained calcite of the surrounding matrix. Such a competency contrast would be suggested by the presence of gaps between the matrix and the ossicle or by oriented mineral growth at the rim of the ossicle. We do not observe either gaps or mineral growths along the margins of the discs, which suggests that the matrix has remained in contact with the ossicle throughout the deformation. Therefore, either the competency contrast is minimal, or, the matrix has undergone a strain that accommodates the shape change of the discs although the fine grain size of the calcite makes it difficult to observe deformation features in the matrix. Our estimates are based on the assumption that strain that is measured from the deformed fossils is a minimum estimate of the plastic strain in the rock.

In those samples which contain both deformed fossils and a cleavage fabric, the flattening plane for the plastic strain is consistently oriented subparallel to the cleavage plane (Fig. 4c). Commonly, the deformed fossils are truncated along solution surfaces and are cross-cut by undeformed calcite-filled veins (Fig. 4d). However, there are also horizons in which the cleavage is well developed and the fossils are undeformed. We interpret these relationships to indicate that the plastic deformation occurred prior to or concurrent with cleavage development, and that both pressure solution and crystal-plastic creep mechanisms were active during an early stage of the deformation. Figure 5 summarizes the typical geometric relationship between cleavage surfaces and deformed fossils.

The strain is inhomogeneous in hand specimen, with discrete zones of high strain surrounding lens-shaped regions of low strain. Finite strain axial ratios determined from fossils lying on bedding planes range from 1:1 to 4:1. Axial ratios for strain at a high angle to bedding also range from no apparent strain to strain ratios of 4:1. These ratios correspond to engineering shortening strains ($l - l_o/l_o$) up to 75%. There is no apparent difference between the magnitude of the strain in the hanging wall and the footwall of the Meade thrust on either bedding planes or profile planes.

The large-scale fold structures in this area have a low axial plunge angle, generally $<10°$, so that down-plunge projections of the structure (Fig. 2b) are nearly vertical and hence approximately parallel to a cross-section containing the transport direction. Strain data from the bedding planes suggest that there is a large component of shortening parallel to the transport direction at the time of cleavage formation and plastic deformation (Fig. 6). These geometric relationships together define the projection plane as a principal plane of strain. Strain markers in the profile plane have an average axial ratio that is slightly larger than axial ratios from bedding plane markers; therefore, we have assumed that the projection

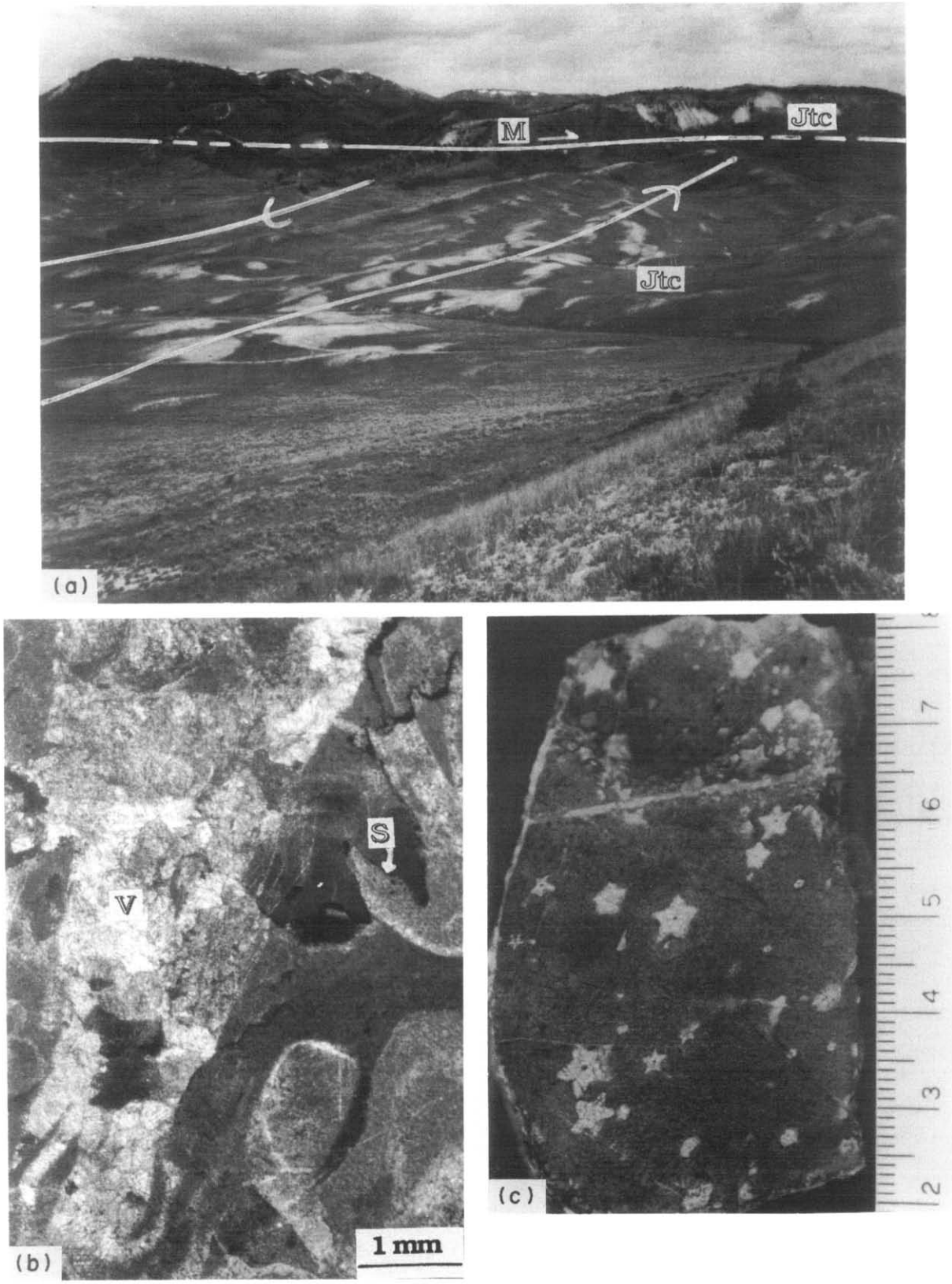

Fig. 3. (a) View looking NNW at exposures of Jurassic Twin Creek Formation (Jtc) in both the footwall and hanging wall of the Meade thrust (M). Traces of footwall folds are indicated. (b) Stylolite surfaces (S), cross-cutting veins (V) and pressure shadows on grains in Twin Creek limestones. (c) Deformed *Pentacrinus* ossicles on bedding plane. Centimeter rule for scale.

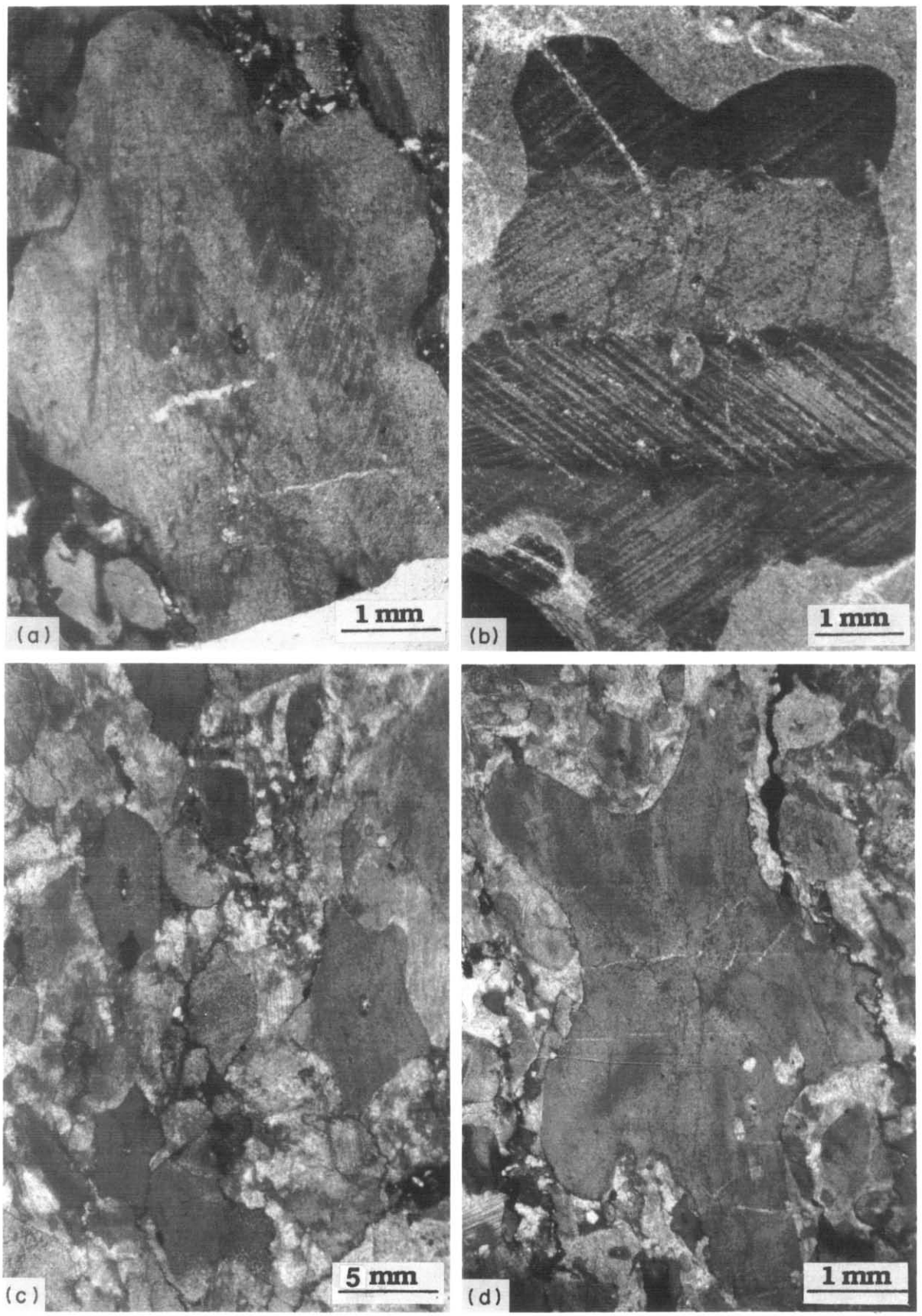

Fig. 4. (a) Photomicrograph of deformed *Pentacrinus* ossicle. The original pentameral symmetry of the ossicle is lost due to plastic deformation. (b) Photomicrograph of a pseudo-deformed *Pentacrinus* which results from oblique cuts through a crinoid column. The oblique cut is indicated by the misorientation of calcite twins across the sutures which separate ossicles in the column. (c) Photomicrograph of strongly deformed *Pentacrinus* ossicles that are truncated by solution selvages (oriented vertically in photograph). The stretching direction for the ossicles is parallel to the flattening plane defined by the solution cleavage. (d) Photomicrograph of deformed ossicle. The fossil is truncated along solution selvages and contains calcite-filled extensional veins. Note absence of gaps between the fossil and the finer grained matrix.

plane approximates the XZ principal plane of strain ($X \geq Y \geq Z$), and that the bedding plane data provide information about the YZ principal plane of strain for the early layer-parallel shortening.

The axial ratio and the orientation of the YZ strain ellipse have been projected from the bedding plane onto the map view for each sample locality (Fig. 6). Strain ellipses in the footwall of the thrust sheet have Y axes that parallel the trend of major N–S folds. In the hanging wall, the orientation of the Y axes shows a greater degree of scatter, although even here, Y axes are oriented approximately perpendicular to the local transport direction.

Figure 7 is a profile section of the folded Jurassic strata in the footwall of the frontal imbricates of the Meade thrust, with strain data superimposed. The plastic strain ellipses have long axes (X) subparallel to the trace of cleavage planes and are oriented at a high angle to bedding. The X axes and cleavage planes fan around each fold, geometrically signifying that both the cleavage and plastic strain stretching direction initiated at a high angle to approximately horizontal bedding and then underwent passive rotation during folding of bedding.

A similar relationship is observed in the profile view of the frontal imbricates of the Meade thrust (Fig. 8b). Although the cleavage–bedding angular relationship has been modified and the cleavage is no longer at a high angle to bedding, the stretching direction for plastic strain is consistently oriented subparallel to the trace of the cleavage seams. The observed relationships between the strain fabric and mesoscopic structures suggest that there is a progressive involvement of an early formed strain fabric into later structures which include both folds and imbricate faults. The modification of original cleavage–bedding relationships in the Meade hanging wall is interpreted to be a result of shearing during the emplacement of the thrust sheet as discussed in the next section.

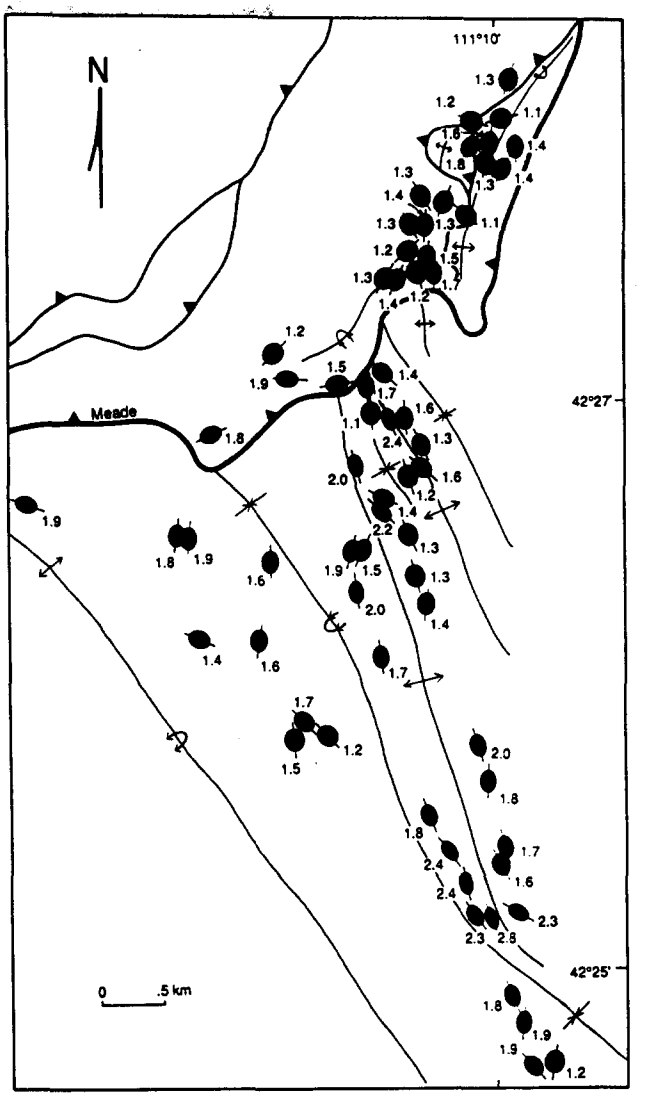

Fig. 6. Strain data obtained from Twin Creek limestones in structures adjacent to the Meade thrust. Numbers represent axial ratios normalized to 1. The form of the strain ellipse is projected from the bedding plane onto map view. The ellipses approximate the YZ principal plane; trends of the Y axes are indicated for each ellipse.

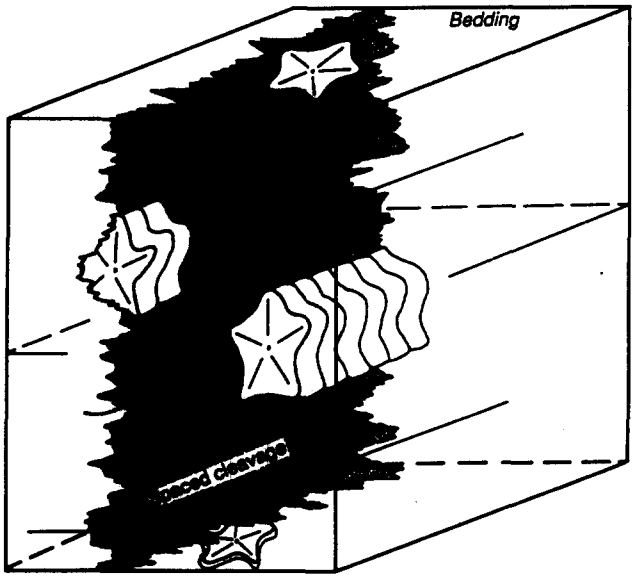

Fig. 5. Block diagram illustrating the geometric relationship between spaced cleavage surfaces (stippled pattern) oriented at a high angle to bedding, and for deformed *Pentacrinus* discs which lie on or at a high angle to bedding plane surfaces. Columns of crinoid discs are randomly oriented on the bedding surfaces.

TIMING OF STRAIN FABRIC AND STRUCTURAL DEVELOPMENT

The Meade thrust places folded Mississippian limestones over a folded sequence of Middle Jurassic and Cretaceous strata. The forelandward progression of thrust faulting between the Meade thrust and the Crawford thrust to the east, is apparent from the folding of the Meade thrust sheet into a broad antiform and synform over a ramp in the underlying thrust (Figs. 2b and 11a). Although the thrust fault is folded, cut-off angles in the

hanging wall and footwall indicate that the Meade thrust followed a flat-lying glide horizon at the base of Mississippian strata and ramped through Pennsylvanian through to Jurassic units to an upper glide horizon in the Jurassic Preuss Formation. The upper and lower glide horizons are now juxtaposed across the fault.

Displacement on the Meade thrust was accompanied by the development of a series of E-verging second-order en échelon folds in the footwall immediately east of the footwall ramp. The fold train is developed above a detachment in the Gypsum Spring Member at the base of the Twin Creek Formation (Coogan & Boyer 1985) and the folds become progressively more upright away from the footwall ramp. Frontal imbricates of the Meade thrust carry sections of an overturned fold limb and truncated fold hinges, indicating that the footwall folds were truncated and overridden by footwall imbricates during emplacement of the thrust sheet (Protzman 1986). The uppermost units of Twin Creek Formation and the shale beds in the overlying Jurassic Preuss Formation are truncated across the hinges of the folds in the footwall (Fig. 7) and are preserved in the hanging wall of minor frontal imbricates (Fig. 8a).

The main frontal imbricate of the Meade thrust carries an overturned section of Triassic through to Jurassic strata in the hanging wall. Both footwall and hanging wall cut-offs for the Jurassic units are exposed in canyon sections that align approximately with the overall transport direction of the thrust sheet (Figs. 2a and 8a & b). At the footwall cut-off locality in Georgetown Canyon (Fig. 8a), the Meade fault forms a structural ramp through the Jurassic units, although the fault surface has been folded subsequently, and the footwall ramp cut-off angle has been modified. Bedding at the footwall cut-off dips steeply toward the west and cleavage is subhorizontal to gently E-dipping. The corresponding hanging wall cut-offs are exposed 10 km southeast of Georgetown Canyon along Preuss Creek (Fig. 8b). The Jurassic strata exposed along Preuss Creek are strongly overturned, dipping 40–70° westward and containing a steeply E-dipping spaced cleavage. In addition to the change in bedding and cleavage orientation between the footwall and hanging wall outcrops, there is a difference in the measured thickness of the Jurassic section, from 1150 m in the footwall to 758 m in the hanging wall. The outcrop width parallel to the fault, however, is approximately constant.

The reduction of the cleavage–bedding intersection angle from 90° (as formed due to early layer parallel shortening) to a more acute angle of 52° (as currently observed in the hanging wall) may be explained as the result of either flexural slip folding or fault parallel shearing (Fig. 9). We interpret the clockwise rotation of the cleavage into a steeper orientation in the hanging wall with respect to the footwall to be the result of fault-parallel shear during the explacement of the thrust sheet (Protzman & Mitra 1985). In addition, top-to-the-east (dextral) shear in the hanging wall will decrease the thickness of any bed with an original westward dip angle, and therefore accounts for the substantial change in thickness of the sheared Jurassic beds in the hanging wall while maintaining a constant width of exposure along the fault (Fig. 10). The imposed simple shear strain may be estimated from the change in bed thickness for the hanging wall of the frontal imbricate relative to the observed footwall geometry (Fig. 10) and gives a shear strain (γ) of 0.85.

The observed relationships between structure and strain fabric indicate that both the footwall and the hanging wall of the Meade thrust were actively deforming concurrent with activity on the main fault surface. The presence of an easy glide horizon at the base of the Twin Creek Formation controlled the sequence of structural development in the footwall and affected the emplacement path of the thrust sheets.

CROSS-SECTION CONSTRUCTION AND RESTORATION

We have constructed a sequence of cross-sections for the Meade thrust sheet using the emplacement sequence deduced from the incremental strain fabric, multiply deformed structures and cross-cutting relationships de-

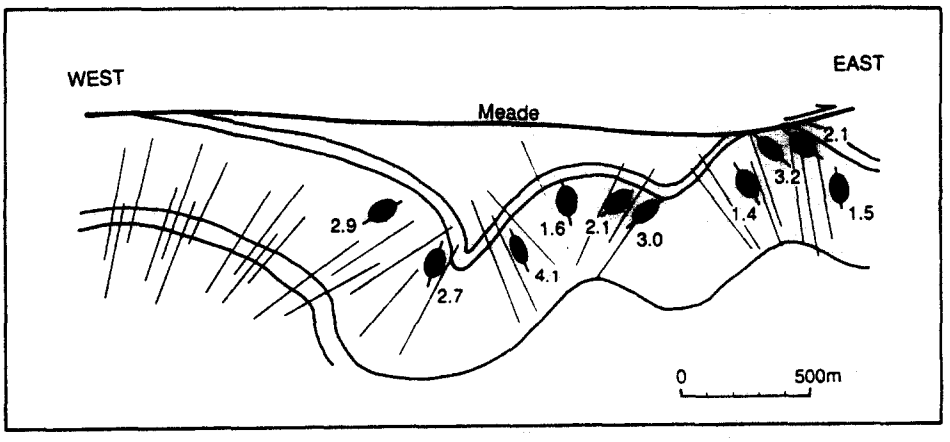

Fig. 7. Down-plunge projection (profile view) of folded Twin Creek strata in the footwall of the Meade thrust. Both cleavage traces and *XZ* strain ellipses are projected onto the profile plane. Numbers represent axial ratios normalized to 1. Trend of projection: 09°/350. Note the truncation of footwall fold hinges by the Meade thrust.

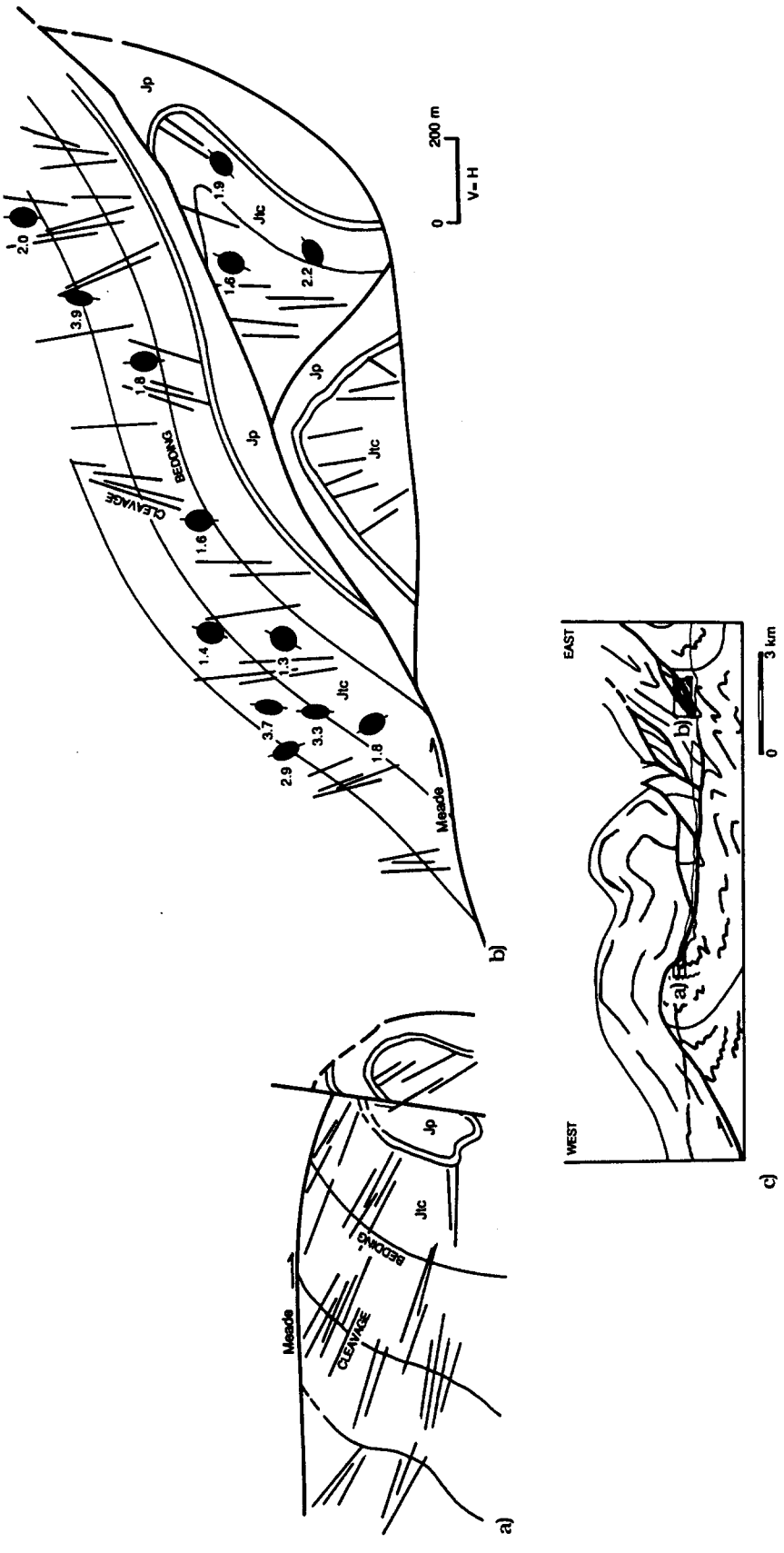

Fig. 8. Geometric relationships between bedding and strain fabric markers along the approximate transport direction of the Meade thrust. (a) and (b) are drawn to same scale. (a) Projected view of Twin Creek bedding cut-offs and cleavage orientation at Georgetown Canyon in the footwall of the Meade thrust. (b) Projected view of Twin Creek bedding cut-offs, cleavage and XZ strain ellipses in the hanging wall of the frontal imbricate of the Meade thrust along Preuss Creek. Note the strong change in orientation of cleavage in the hanging wall with respect to (a). (c) Simplified cross-section of the Meade thrust showing relative locations of (a) and (b). The Georgetown Canyon and Preuss Creek localities (Fig. 2a) are projected from the north and south (respectively) onto the cross-section plane and do not lie in an exact transport plane.

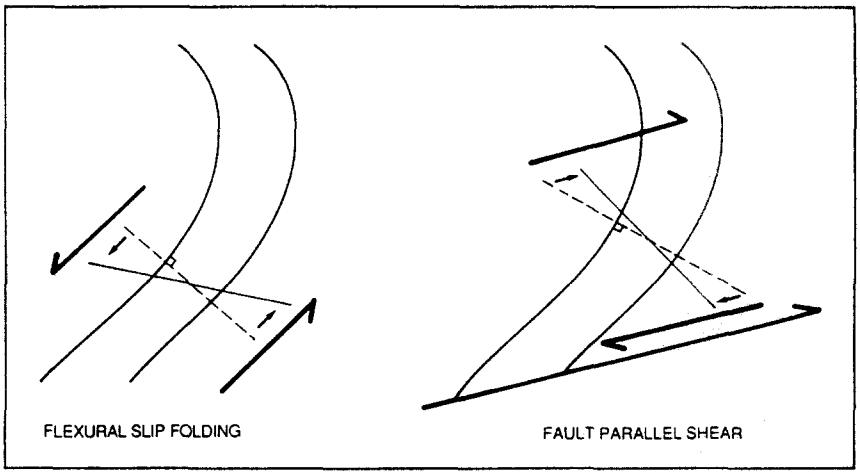

Fig. 9. Comparison of the effect of flexural slip folding and fault parallel shear on the orientation of an original bed-normal cleavage. The bed-normal cleavage (dashed line) becomes more shallowly dipping (solid line) in the case of flexural slip in the limb of a fold, and more steeply dipping (solid line) if rotated due to shear deformation in the hanging wall of a fault. Compare fault parallel shear reorientation geometry with Fig. 8(b).

scribed above. At each step in the geometric retrodeformation, matching footwall and hanging wall cut-offs and truncated structures are restored and the appropriate increments of strain are removed. If a distinct sequence of deformation is evident, as is the case for the Meade thrust sheet, or, if an 'out of sequence' faulting event has been recognized, the order of the deformation reversal becomes significant for the interpretation of successive sections.

Five stages of retrodeformation

Five stages in the retrodeformation and balancing of the Meade cross-section are discussed below. Where appropriate, we give details of the methods used to incorporate the strain fabric and other structural analyses as kinematic and geometric constraints. For the rest of the balanced cross-section construction we use standard techniques of cross-section balancing (Woodward *et al.* 1985).

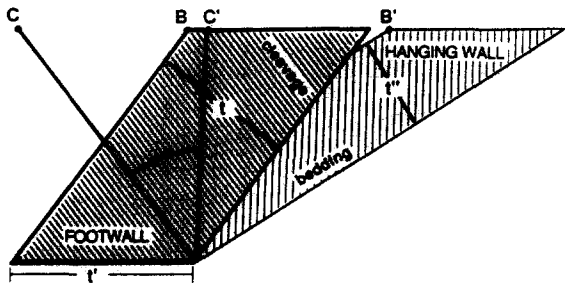

OBSERVED: (in HW)
BEDDING ^ CLEAVAGE = 52°
FAULT ^ BEDDING (α') = 31°
BED THICKNESS (t'') = 758 m
WIDTH OF BEDDING ALONG FAULT (t') = 1455 m
$t' = t''/\sin \alpha'$

KNOWN: (IN FW)
ORIGINAL BED THICKNESS (t) = 1150 m

CALCULATED:
ORIGINAL FAULT ^ BEDDING (α) = 52°
$\alpha = \sin^{-1} t/t'$
ORIGINAL BEDDING ^ CLEAVAGE = 73°
ANGULAR SHEAR STRAIN (Ψ) = 40.5°
SHEAR STRAIN (γ) = 0.85

Fig. 10. Calculation of the increment of simple shear parallel to the fault, based on measured exposures. Parallelograms represent the footwall and hanging wall geometries of portions of the Twin Creek Formation.

Stage 0 (Fig. 11a). We begin our restoration with a cross-section that is constructed as a composite of downplunge projections of the structure adjacent to the Meade thrust, based on new field data (Protzman 1986) and published maps (Cressman 1964). The section is also constrained by subsurface information from published cross-sections (Dixon 1982, Coogan & Yonkee 1985).

Stage 1 (Fig. 11b). The section is pinned on the lowermost thrust present in the section (Tunp thrust) and the folded and faulted strata of the Crawford thrust sheet and associated minor imbricates (including the Sheep Creek thrust) are restored to horizontal. The lack of superimposed strain fabrics within the Meade thrust sheet, suggests that internal strain during the piggyback transport of the Meade sheet on the Crawford thrust system is minimal, and therefore standard line length and area balancing techniques can be applied (Woodward *et al.* 1985).

After this stage of the retrodeformation, the trajectory of the Meade thrust fault has been restored to the approximate geometry that preceded motion on the underlying faults. Note that the folds within the Jurassic strata are still present and will remain in the section until after the displacement on the Meade thrust has been restored.

Stage 2 (Fig. 11c). Displacement on the main frontal imbricate of the Meade thrust is restored by matching bedding cut-offs for the thinned and overturned Jurassic and Triassic strata across the fault surface. The increment of shear strain parallel to the fault ($\gamma = 0.85$) that was calculated earlier (Fig. 10) is restored to the hanging

wall at this stage in the restoration. Several minor horses and adjustment faults within the hanging wall are also restored at this step. The frontal imbricates of the Meade thrust carry sections of an overturned fold limb and truncated portions of fold hinges. Therefore, when the displacement on each frontal imbricate is removed in the correct sequence, the footwall geometry restores to that of an asymmetric E-verging fold train.

This stage in the restoration results in a section which shows the restored footwall fold train and the presence of a major overturned synformal hinge in the footwall adjacent to the Meade fault. Examination of the section suggests a particular sequence of activity between the two main imbricates of the Meade fault (labelled 1 and 2). The geometric restoration to a large overturned syncline requires that translation on imbricate 1 be associated with the development of both the overturned footwall syncline and frontal fold train prior to motion on imbricate 2, as imbricate 2 is the fault that truncates the hinge regions of these folds.

Stage 3 (Figs. 11d & e). The next increment of deformation to be factored out of the cross-section is the folding within the Twin Creek and Preuss strata in the footwall of Meade fault 1. The geometry of the N-plunging fold train is based on short-range down-plunge projections as in Fig. 7. The folds are developed above the Gypsum Spring detachment at the base of the Twin Creek Formation (Coogan 1985), and hence the depth of folding is well constrained. Line length and area balancing techniques are used to restore the folded strata to horizontal and the cleavage to a general N–S trend and vertical orientation. Note that two blind thrusts in the footwall of the Meade thrust originally terminated in the folded Twin Creek Formation. These thrusts will restore to steep trajectories within the restored strata. Uncertainty regarding their restored geometry is indicated by dashed lines in the final restoration. Due to the lack of available constraints on the restored trajectories for these faults, they are not shown in the intervening stages. Next, the overturned footwall syncline is unfolded in a zone of simple shear parallel to the fault and bounded by the hinge region of the fold.

Stage 4 (Fig. 11e). To this stage in the retrodeformation, the Upper Jurassic section has restored to an anomalously thick stratigraphic package that reflects the early layer-parallel shortening and vertical thickening of the strata. Because the total layer-parallel shortening consists of contributions from both the pressure solution and plastic strain, cleavage planes and strain ellipses that served as kinematic markers in previous steps of the restoration are now used to adjust the stratigraphic thickness of the Jurassic Twin Creek section.

Based on the strain fabric, an increase in the line lengths that bound the Twin Creek Formation is needed to account for an estimated average of 10% pressure-solution strain in the frontal parts of the Crawford sheet and a combination of 15% pressure solution strain and 20% plastic strain in the strata that presently occupy positions in the footwall and hanging wall of the Meade thrust (Fig. 11e).

Stage 5 (Fig. 11f). At this stage, having restored all known increments of strain and displacement to the section, we observe that the trajectory of the Meade thrust fault does not restore to a conventional ramp and flat geometry. The shape of the fault trajectory reflects the fact that the fault transected a deforming footwall during emplacement of the thrust sheet. We indicate our uncertainty of the fault trajectory at depth and to the west with a dashed line. Any internal deformation of the Lower Paleozoic units would affect the position of the fault trace, but the lack of exposures of these units hampers our ability to constrain the magnitude of the deformation in these subsurface units. The shaded area represents the range of possible fault paths at depth, allowing for 0% strain (steep ramp) to strain equalling that of the Jurassic strata (shallow ramp). In addition, uncertainty regarding the trajectory of blind thrust faults which lose slip within the previously shortened, thickened and folded Twin Creek strata is indicated by dashed lines in the restoration. Such faults can not be restored to an accurate pre-thrusting trajectory because they cannot be pinned to an exact point within the previously deformed layer. Therefore, it is apparent that this is the last stage in the reconstruction that can be defined with any certainty.

DISCUSSION

We have constructed a series of partially restored sections to reflect the emplacement history of the Meade thrust sheet in the Idaho–Wyoming thrust belt, based on structural analyses of the strain fabric that is preserved in both the hanging wall and footwall of the thrust sheet, in addition to cross-cutting relationships and truncated structures. The geometric and kinematic data are used to construct a series of intermediate steps reflecting the progressive internal deformation of the thrust sheet during motion on the Meade thrust and its imbricates. Although bed lengths are not consistent between the deformed state and the final restored section the inconsistencies in these measurements and their causes are explained in the intermediate sections.

There are limitations to the ability to draw a balanced cross-section in a complexly deformed terrain which stem from our lack of information regarding subsurface décollement horizons, degree of involvement in thrust structures at depth and the amount of penetrative deformation in units not exposed at the surface. Hence, the final section shown in our restoration (Fig. 11f) must be considered to be only partially balanced as the effects of ductile deformation in the units at depth can only be estimated. As a direct consequence, the fault trace can not be pinned and therefore cannot be used as a reference point for reconstructions further into the hinterland.

We have used the strain data that can be obtained

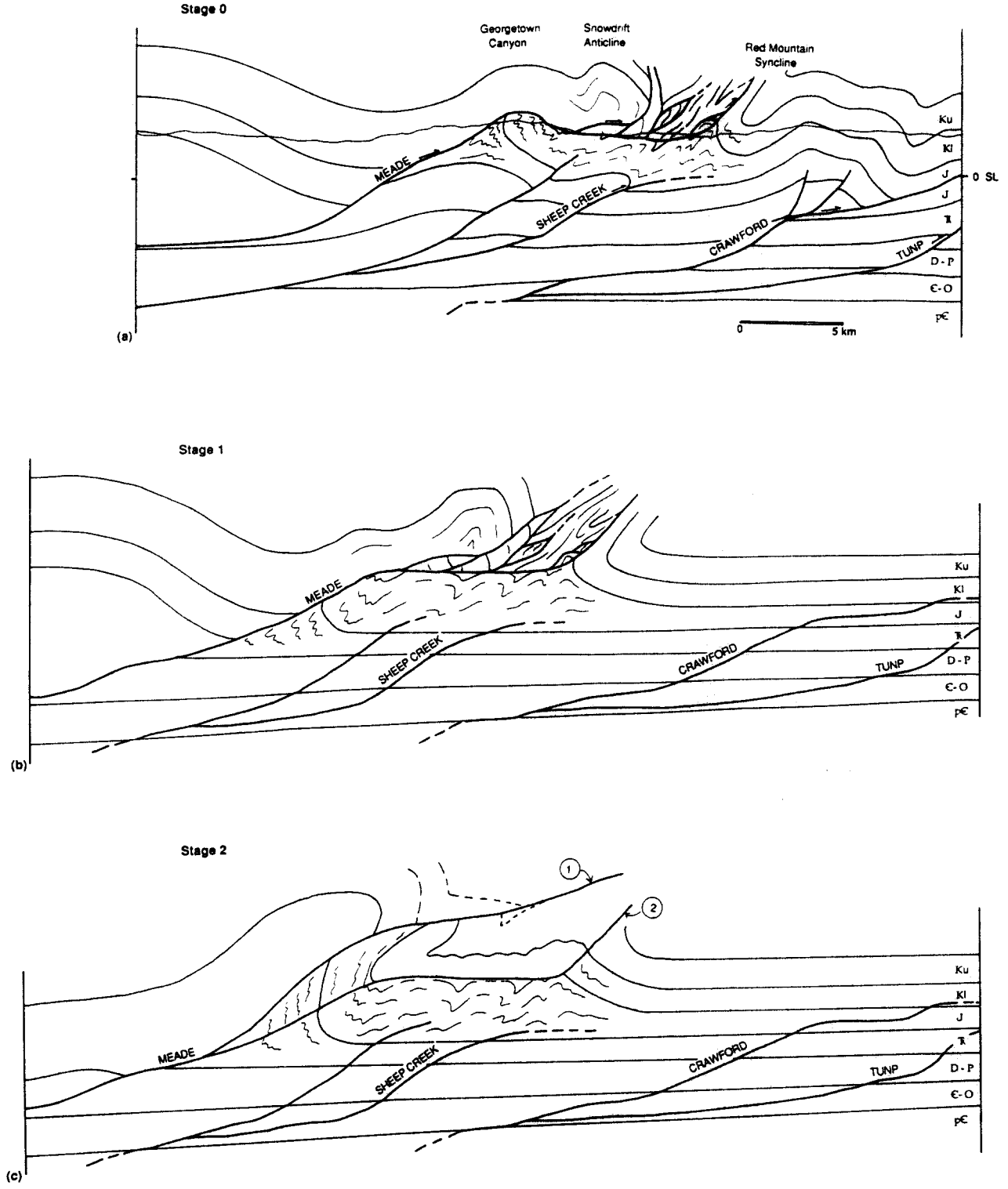

Fig. 11(a)–(c).

from the area adjacent to the section line, not to restore individual finite elements to an undeformed state, an impractical if not impossible task, but rather, to characterize both the regional and local characteristics of the strain fabric and the history of its development. The ultimate goal of incorporating this additional information is to develop a method in which section construction itself becomes a tool for analyzing structural data. For example, new information regarding the emplacement history of the Meade thrust sheet that can be derived from various stages in the restored cross-section includes the following. (1) Significant deformation in the form of both folding and slip on minor décollements occurred within the footwall of the Meade thrust at the time of emplacement of the Meade thrust sheet (Figs. 11d & e). This deformation represents the earliest increment of thrust-related deformation within the next incipient thrust sheet, but it is completely unrelated to motion on the underlying thrust. (2) There is a significant control on the structural development of both the

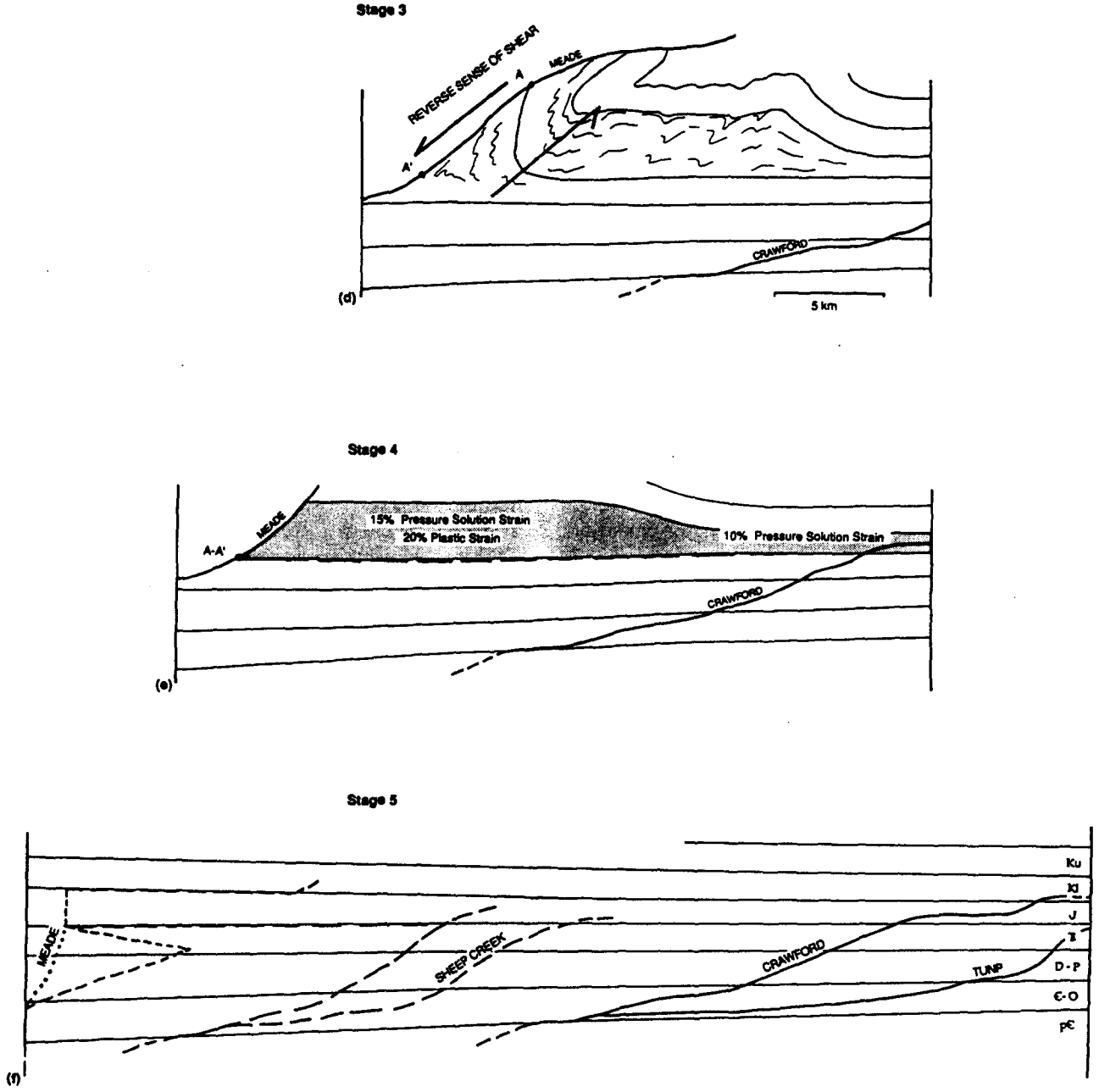

Fig. 11. Series of cross-sections illustrating the stages required for the retrodeformation of a cross-section containing the Meade thrust sheet. All sections and intermediate steps are drawn at the scale given for Stage 0. Each stage in the retrodeformation is described in the text.

hanging wall and footwall of the thrust sheet by the lithologic package. The presence of an easy glide horizon at the base of the thick sequence of Twin Creek limestones allows differential shortening to occur above the horizon through cleavage development and folding, while strata beneath the décollement remain relatively undeformed (Figs. 11d & e). (3) It is possible to determine the relative timing of individual imbricates of the thrust system based on the formation and truncation of individual structures. As shown in Fig. 11(c), a large overturned fold limb and an E-verging fold train are successively truncated by a leading imbricate of the basal thrust. The formation of the fold structures is related to motion on an earlier imbricate thereby constraining a time sequence between the two faults. (4) Imbricate 1 (Fig. 11c) carries Mississippian rocks over folded Jurassic strata and is therefore the main slip surface of the Meade thrust system. Imbricate 2 has relatively minor displacement as a footwall splay within Triassic and Jurassic strata. It is important to note that on most geologic maps, however, the trace of imbricate 2 is labelled as the frontal position of the Meade thrust sheet. (5) Both the reorientation of the strain fabric and the thinning of hanging wall units (Figs. 8, 9 and 10) are evidence for an increment of shear deformation parallel to the fault during the actual emplacement of the thrust sheet. Such geometric changes need to be accounted for in the balancing of the cross-section as they affect the

geometry of cut-off angles and bed thicknesses that are used in the construction. (6) Finally, it is apparent that the restored fault trace (Fig. 11e), for an area in which footwall deformation accompanied emplacement of the sheet, will not reflect the actual movement path of the propagating thrust fault and therefore should not be expected to restore to a typical thrust fault configuration.

The selection of a technique for the restoration of a strain increment into a cross-section should be influenced primarily by the characteristics of the individual strain fabric (see also a review by Woodward *et al.* 1986). We have discussed an example in which the strain fabric can be correlated to an early stage in the deformation event, and therefore the strain fabric can be used as a kinematic marker throughout the section reconstruction prior to its restoration in the section. It is apparent that a strain fabric which forms early in a deformation event, and is retained in the rock without major modification, can be used as a bridging constraint between initial, intermediate and final geometries. In this case, the recognition of a systematic relationship between the early strain fabric and other early structures aids the interpretation. The early formed fabric should restore to its presumed initial position in the final restored section, providing an additional check on the viability of the restoration.

Other types of strain fabrics developed in other areas may require different techniques for incorporation into balanced sections. For example, strain fabrics that show evidence for continuous development throughout a deformation are best restored with an integration method that can spread the strain increment over the total time history of the deformation. In practice, however, it is difficult to combine algebraic integration procedures into a geometric construction. Until such techniques are more readily available, this integration will continue to be approximated by a one-step total-strain reversal. The drawback to such a simplification is that a one-step strain reversal can lead to the construction of a restored section that does not reflect any actual stage in the deformation event, and thus leads to an incorrect 'balanced section'.

There are some strain fabrics whose development can be correlated with a fairly limited range of deformation and metamorhic conditions; these must be treated as representing only a portion of the total strain in the rock. To be precise, the increment of strain represented by this type of strain fabric should be factored into the retrodeformation at the exact stage in the structural development that corresponds to those conditions. Conversely, it is possible for a single strain increment to be represented by several different strain fabrics, particularly in different lithologies, each forming in response to the mechanical behavior of individual lithotectonic units. It is clear, then, that the use of strain fabrics in the retrodeformation of cross-sections relies on our ability to differentiate between individual strain increments and/or to relate equivalent strains which are represented by different strain fabrics in different lithologies. Finally, to achieve kinematic and geometric validity in the various stages of the restored section, the development of the strain fabric must be linked to the appropriate stages in the deformation.

CONCLUSION

We have presented a partially restored cross-section of the Meade thrust sheet, an internal sheet of the Idaho–Wyoming fold and thrust belt. This reconstruction is based on a detailed structural study of a small but relatively well-exposed portion of the Idaho–Wyoming thrust belt. To a large degree the deformation associated with the emplacement of the Meade thrust sheet was affected by the nature of the stratigraphic package, and the extent of footwall deformation appears to be a function of the position of detachment horizons (e.g. the Gypsum Spring Member of the Twin Creek Formation). Because the nature of the stratigraphic package varies strongly over short distances in the thrust belt, it is difficult to generalize the results of this study to other internal thrust sheets. In addition to the stratigraphic sequence, other factors may be significant for the early deformation of the incipient footwall rocks. For example, it is not yet understood what effect the incorporation of crystalline basement rocks in the hanging wall of internal thrust sheets, or the spacing, duration and rate of motion of adjacent thrust faults will have on the geometry and deformation of the growing thrust wedge.

The reconstructed section incorporates detailed structural history, strain and incremental strain information into a step-wise restoration of the Meade sheet. Such an incremental retrodeformation may be the only way of drawing viable sections in complexly deformed internal sheets, and points out the pitfalls of making simplifying assumptions in these areas. The method also points out the possibility of using detailed, retrodeformable sections as tools in understanding complex thrust-emplacement histories.

Acknowledgements—This research was supported by NSF grant EAR-8507039 to G. Mitra, and by grants from the Geological Society of America, Sigma Xi, and the University of Rochester to G. Protzman. The contents of this paper benefitted from discussions with participants of the Penrose conference on the construction of balanced cross-sections, and from thoughtful reviews by N. Woodward, D. Wiltschko and S. Treagus.

REFERENCES

Armstrong, F. C. & Oriel, S. S. 1965. Tectonic development of the Idaho–Wyoming thrust belt. *Bull. Am. Ass. Petrol. Geol.* **49**, 1847–1866.

Armstrong, R. L. 1968. Sevier orogenic belt in Nevada and Utah. *Bull. geol. Soc. Am.* **79**, 429–458.

Coogan, J. & Boyer, S. E. 1985. Variable shortening in fold-thrust belts and implications for cross-section balancing: an example from the Idaho–Wyoming thrust belt. *Geol. Soc. Am. Abs. w. Prog.* **17**, 552.

Coogan, J. & Yonkee, W. A. 1985. The Jurassic Preuss salt detachment in the Idaho–Wyoming thrust belt. *Utah Geol. Ass.* Publ. 14, 75–82.

Cooper, M. A. & Trayner, P. M. 1986. Thrust-surface geometry:

implications for thrust-belt evolution and section-balancing techniques. *J. Struct. Geol.* **8**, 305–312.
Cressman, E. R. 1964. Geology of the Georgetown Canyon–Snowdrift Mountain area, southeastern Idaho. *Bull. U.S. geol. Surv.* **1155**.
Cutler, J. & Elliott, D. 1983. The compatibility equations and the pole to the Mohr circle. *J. Struct. Geol.* **5**, 287–297.
Dahlstrom, C. D. A. 1969. Balanced cross-sections. *Can. J. Earth Sci.* **6**, 743–757.
Dixon, J. S. 1982. Regional structural synthesis, Wyoming salient of the western overthrust belt. *Bull. Am. Ass. Petrol. Geol.* **66**, 1560–1580.
Evans, J. P. & Craddock, J. P. 1985. Deformation history and displacement transfer between the Crawford and Meade thrust systems, Idaho–Wyoming overthrust belt. *Utah Geol. Assoc. Publ.* **14**, 83–95.
Gentry, D. J. 1983. Solution cleavage in the Twin Creek Formation and its relationship to thrust fault motions in the Idaho–Wyoming thrust belt. Unpublished M.S. thesis, University of Wyoming.
Imlay, R. W. 1967. Twin Creek Limestone (Jurassic) in the western interior of the United States. *Prof. Pap. U.S. geol. Surv.* **540**.
Mitra, G. & Yonkee, W. A. 1985. Relationship of spaced cleavage to folds and thrusts in the Idaho–Utah–Wyoming thrust belt. *J. Struct. Geol.* **7**, 361–373.
Mitra, G., Yonkee, W. A. & Gentry, D. J. 1984. Solution cleavage and its relationship to major structures in a fold and thrust belt. *Geology* **12**, 354–358.
Protzman, G. 1986. The emplacement and deformation history of the Meade thrust sheet, southeastern Idaho. Unpublished M.S. thesis, University of Rochester.
Protzman, G. M. & Mitra, G. 1985. Emplacement history of a thrust sheet based on analysis of pressure solution cleavage and deformed fossils. *Geol. Soc. Am. Abs. w. Prog.* **17**, 694.
Ramsay, J. G. & Huber, M. I. 1983. *The Techniques of Modern Structural Geology. Volume* 1: *Strain Analysis*. Academic Press, New York.
Royse, F., Warner, M. A. & Reese, D. L. 1975. Thrust belt structural geometry and related stratigraphic problems, Wyoming, Idaho, northern Utah. *Rocky Mountain Association Geologists Symposium*, 41–54.
Rubey, W. W. & Hubbert, M. K. 1959. Role of fluid pressure in mechanics of overthrust faulting: II. Overthrust belt in geosynclinal area of western Wyoming in light of fluid pressure hypothesis. *Bull. geol. Soc. Am.* **70**, 167–206.
Stockdale, P. B. 1926. The stratigraphic significance of solution in rocks. *J. Geol.* **34**, 399–414.
Treagus, S. H. 1987. Mohr circles for strain, simplified. *Geol. J.* **22**, 119–132.
Wiltschko, D. V. & Dorr, J. A., Jr. 1983. Timing of deformation in the overthrust belt and foreland of Idaho, Wyoming and Utah. *Bull. Am. Ass. Petrol. Geol.* **67**, 1304–1322.
Woodward, N. B., Boyer, S. & Suppe, J. 1985. An outline of balanced cross-sections. University of Tennessee Dept Geol. Science. *Studies in Geology* 11 (2nd edn).
Woodward, N. B., Gray, D. R. & Spears, D. B. Including strain data in balanced cross-sections. *J. Struct. Geol.* **8**, 313–324.
Yonkee, W. A. 1983. Mineralogy and structural relationships of cleavage in the Twin Creek Formation within part of the Crawford thrust sheet in Wyoming. Unpublished M.S. thesis, University of Wyoming.

APPENDIX

Determination of two-dimensional strain from Pentacrinus

An undeformed *Pentacrinus* (Fig. A1a) has a pentameral symmetry consisting of five rays that are oriented around a central column. In the undeformed state, each ray is the perpendicular bisector of the two adjacent rays (Fig. A1a). During deformation the rays rotate toward the principal stretching direction and the angles between rays change. The angular shear (ψ), which is defined as the angular deflection between two initially perpendicular lines (Ramsay & Huber 1983), can be measured for any three adjacent rays using ray orientations obtained from camera lucida sketches (Fig. A1b). The Mohr circle for two-dimensional strain (Fig. A1c) can be constructed using angular shear measurements from any two ray directions, and can be checked for homogeneity using the five measurements of angular shear that can be determined from each fossil.

Steps in the Mohr circle construction (after D. Elliott class notes, 1973) are:

(1) Measure the angular shear strain and orientation for at least two rays from the deformed disc.

(2) On graph paper, draw a vertical line representing the orientation of ray A′ in the physical plane. This is the λ'_A line in the Mohr circle plane.

(3) Choose any point along λ'_A and label the point A′.

(4) From A′ draw a line having the angle ψ_A with the horizontal. Note the sign convention for this construction of the Mohr plane: clockwise shear plots upward (see also Treagus 1987).

(5) Choose the origin of the strain plane to the left of point A′ and along the line constructed in step (4). Draw the horizontal axis to include this point and be perpendicular to the λ'_A line.

(6) The Pole to the Mohr circle (Cutler & Elliott 1983) lies symmetrically opposite strain point A′ along line λ'_A (i.e. at the same distance as A′ across the horizontal axis). Label the Pole P.

(7) Through the Pole draw the line parallel to the physical orientation of the second ray B′. The angle between λ'_A and this new line should be equal to and in the same relative position as the angle between rays A′ and B′ in the physical plane.

(8) From the origin of the strain plane, draw the line representing the angular shear strain for ray B′. The intersection of this line and the line representing the physical orientation of ray B′ is the strain point B′.

(9) The perpendicular bisector of chord A′B′ intersects the horizontal (λ') axis at the origin of the Mohr circle.

(10) Use the radius to complete the construction of the Mohr circle.

(11) Lines connecting the Pole to λ'_1 and λ'_2 of the Mohr circle are parallel to the orientations of λ_1 and λ_2 in the physical plane (Fig. A1b) and can be transferred to the physical plane directly.

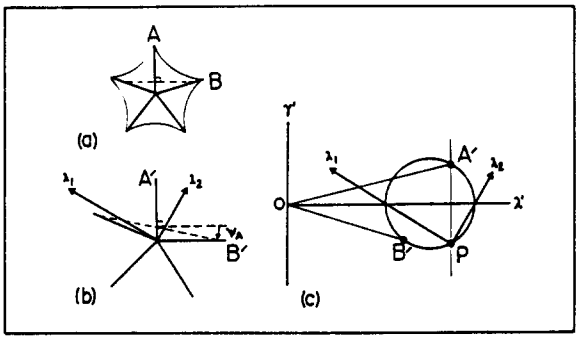

Fig. A1. Geometric relationships and Mohr circle construction for the determination of two-dimensional strain from deformed *Pentacrinus* ossicles. (a) Undeformed *Pentacrinus* in which each ray is the perpendicular bisector of the two adjoining rays. (b) Deformed *Pentacrinus* showing changes in the angular relationship between rays. (c) Mohr circle construction and determination of the orientation of the principal axes of strain. Details of the method are given in the Appendix. Strain axes can be directly transferred from the Mohr circle construction to the plane of the deformed ossicle.